13 October 2000

ELSEVIER

Chemical Physics Letters 329 (2000) 29–35

CHEMICAL PHYSICS LETTERS

www.elsevier.nl/locate/cplett

Rotationally resolved A $^2\Pi_u \leftarrow$ X $^2\Pi_g$ electronic spectrum of tetraacetylene cation

David Pfluger, Tomasz Motylewski, Harold Linnartz, Wayne E. Sinclair *, John P. Maier

Institute for Physical Chemistry, University of Basel, Klingelbergstrasse 80, CH 4056 Basel, Switzerland

Received 25 July 2000; received in final form 22 August 2000

Abstract

The rotationally resolved A $^2\Pi_u \leftarrow$ X $^2\Pi_g$ electronic origin band spectrum of tetraacetylene cation (HC_8H^+) and its deuterated derivative (DC_8D^+) has been recorded in the gas phase, applying both frequency modulation spectroscopy in a liquid nitrogen cooled hollow cathode discharge and cavity ringdown spectroscopy in a supersonic planar plasma. The combined analysis of the rotational structure yields accurate molecular constants for the ground and electronically excited states as well as information on the molecular geometry. © 2000 Elsevier Science B.V. All rights reserved.

1. Introduction

The radical cations of the polyacetylene series are considered to be important intermediates in plasma and combustion reactions. Members of the series $HC_{2n}H^+$ with $n = 2$–4 have been a subject of previous spectroscopic studies in the gas phase [1–7]. The first electronic spectrum of a polyacetylene cation was obtained by Schüler and Reinbeck [1] and was assigned by Callomon [2] to the A $^2\Pi_u \rightarrow$ X $^2\Pi_g$ electronic origin band transition of the diacetylene cation. In two subsequent studies, the absolute rotational numbering of HC_4H^+ was discussed and all bond lengths in both electronic states were determined [4,5]. The A $^2\Pi_g \rightarrow$ X $^2\Pi_u$ electronic spectrum of triacetylene cation was initially recorded in emission by Allan et al. [6] and recently the A $^2\Pi_g \leftarrow$ X $^2\Pi_u$ origin band was rotationally resolved and analysed using frequency modulation (FM) absorption measurements [7]. As far as the tetraacetylene cation is concerned, little is known up to date. The A $^2\Pi_u \rightarrow$ X $^2\Pi_g$ electronic spectrum was observed in the gas phase in an emission spectrum employing low-energy electron impact excitation on an effusive beam [3].

In this work, the rotationally resolved absorption spectrum of the A $^2\Pi_u \leftarrow$ X $^2\Pi_g$ origin band transition of HC_8H^+ in the gas phase is presented. The spectra were recorded using two complementary experimental approaches with different types of ion sources. These are FM spectroscopy of rotationally cooled HC_8H^+ in a hollow cathode discharge at about 150 K and cavity ringdown (CRD) spectroscopy of the ion rotationally cooled in a supersonic planar expansion to about 15 K, yielding to spectra with significantly different rotational profiles. Although the FM spectra were obtained at high resolution to resolve clearly the rotational structure, it was not possible to determine unambiguously the absolute numbering in

* Corresponding author. Fax: +41-61-267-3855.
E-mail address: wayne-e.sinclair@unibas.ch (W.E. Sinclair).

0009-2614/00/$ - see front matter
PII: S0009-2614(00)00976-3

the rotational analysis. On the other hand the CRD spectra were measured at lower resolution, but changes in the rotational profile on cooling the ions to very low rotational temperatures allowed the appearance of the distinct Q branch to be identified and an absolute numbering to be established.

2. Experimental

2.1. FM-discharge modulation in a hollow cathode plasma

The experimental approach has been described [7]. Gas mixtures of 0.5% diacetylene in helium or 1% dideuteroacetylene in neon were used for the production of HC_8H^+ and DC_8D^+ in a liquid nitrogen cooled hollow cathode discharge that is incorporated into a multiple reflection cell. The production was modulated at 12–14 kHz by an amplified and rectified AC voltage.

The output of an Ar^+ pumped cw Ti:S ring laser operating near 700 nm was electro-optically modulated at a radio frequency of 192 MHz. The light multipasses the plasma in a White-type geometry yielding an effective optical pathlength of ~100 m and is focused onto a fast photodiode. The high-frequency portion of the signal is demodulated in a double balanced mixer that was referenced to the radio frequency that drives the electro-optic modulator. The photodiode signal was fed to a lock-in amplifier which demodulated the signal at the discharge modulation frequency. As a result of the FM process the absorption bands show a derivative-like shape. An absolute frequency calibration was obtained by simultaneously recording an iodine reference gas spectrum. Typical rotational temperatures are 150 K.

2.2. CRD in a supersonic planar plasma

The experimental method has been described [8]. A supersonic planar plasma was generated by discharging a high pressure gas pulse (30 Hz repetition rate, 10 bar backing pressure) of a 0.25% acetylene or dideuteroacetylene in a helium mixture in the throat of a 3 cm × 300 μm slit nozzle. Adiabatic cooling yields a rotational temperature around 15 K. A standard CRD spectrometer was used to detect the signals in direct absorption. The laser bandwidth is ~0.03 cm^{-1} using an étalon in the dye laser cavity. The data were calibrated and linearized using an external wavemeter.

3. Results and discussion

For a $^2\Pi \leftarrow {}^2\Pi$ electronic transition of a linear molecule one expects to observe two separate bands (each consisting of a P, Q and R branch) that correspond to the parallel transitions between the two spin orbit components, $^2\Pi_{3/2} \leftarrow {}^2\Pi_{3/2}$ and $^2\Pi_{1/2} \leftarrow {}^2\Pi_{1/2}$. This has been similarly observed for other polyacetylene cations [5,7]. The intensity ratio of the two bands is determined by the 'spin–orbit temperature' – generally close to T_{rot} – and the value of the spin–orbit splitting in the ground state (A''). In the case of HC_8H^+ the $X^2\Pi_g$ and $A^2\Pi_u$ states are described by the electronic configurations $\ldots(\pi_u)^4(\pi_g)^3$ and $\ldots(\pi_u)^3(\pi_g)^4$, respectively, and thus the states are inverted ($A'' < 0$), i.e., the $\Omega = 3/2$ lies energetically below $\Omega = 1/2$. The splitting between the two components is given by the difference in spin–orbit constants in ground and excited states ($|A'' - A'|$) and is expected in analogy with HC_6H^+ to be of the order of a few wavenumbers.

Part of the $A\,^2\Pi_u \leftarrow X\,^2\Pi_g$ electronic origin band transition of HC_8H^+ recorded in the discharge cell is shown in Fig. 1. In the range 14 135–14 147 cm^{-1} a resolved rotational structure with rovibronic linewidths of ~350 MHz (FWHM) is observed. The corresponding translational temperature ~150 K is in agreement with the value determined from the band intensities. The spectrum consists of two bands that correspond to the parallel $A\,^2\Pi_{3/2} \leftarrow X\,^2\Pi_{3/2}$ and $A\,^2\Pi_{1/2} \leftarrow X\,^2\Pi_{1/2}$ transitions. The red-shaded band head belonging to the $R_{3/2}$ branch is clearly visible, whereas the $R_{1/2}$ band head that is shifted 3 cm^{-1} to lower energy is barely visible due to strong overlap with the most intense region of the $P_{3/2}$ branch. For the same reason it is much easier to discern rotational lines in the $\Omega = 3/2$ than in

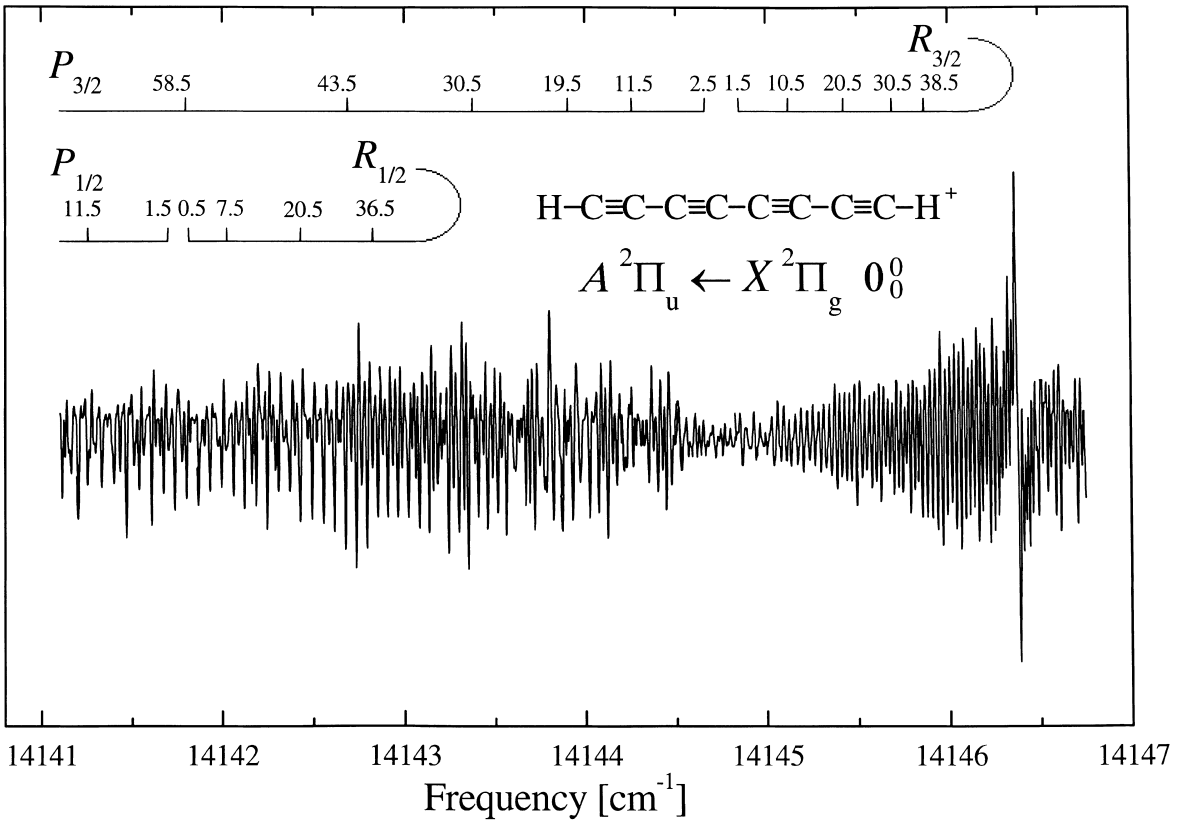

Fig. 1. Rotationally resolved FM absorption spectrum of the $A\,^2\Pi_u \leftarrow X\,^2\Pi_g\ 0_0^0$ band of HC_8H^+ in a liquid nitrogen cooled hollow cathode discharge of a mixture of C_2H_2 in He ($T_{rot} \approx 150$ K). The rotational assignment of the subbands is indicated. The instrumental lineshape is approximately first derivative, due to the modulation scheme employed.

the $\Omega = 1/2$ component. Furthermore, it is not possible to locate the Q-branch positions from this data set. At the high ambient temperatures in the cell a population distribution over many rotational levels is expected and thus transitions at low J are not readily identified which leads to ambiguity in the absolute numbering of the rotational lines. In addition, for electronic transitions with $\Delta\Lambda = 0$, the Q-line strength S_{JJ} is given by $S_{JJ} = \Omega^2(2J+1)/(J(J+1))$ and is only expected to be of significant intensity at low temperatures. In a supersonic expansion these problems are overcome.

Fig. 2 shows the same spectral region as in Fig. 1 recorded by CRD in the slit jet experiment. The spectrum is the smoothed average of several independent scans. Only one subband, the $A\,^2\Pi_{3/2} \leftarrow X\,^2\Pi_{3/2}$ component, is clearly visible. As the ground state spin–orbit splitting is expected to be of the order of 30 cm^{-1}, the population of the higher spin–orbit component will be only moderate at the low temperature in the jet. In addition, the $A\,^2\Pi_{1/2} \leftarrow X\,^2\Pi_{1/2}$ band will be partly hidden under the P-branch of the $\Omega = 3/2$ component. At the low rotational temperature of 15 K the identification of the Q branch at 14 144.68(1) cm^{-1} for HC_8H^+ and at 14 171.02(1) cm^{-1} for DC_8D^+ becomes possible as well as an assignment of the lower rotational transitions. The absolute numbering of the lines with high J values in the $A\,^2\Pi_{3/2} \leftarrow X\,^2\Pi_{3/2}$ subband recorded in the cell was decided by considering the position of the Q-branch maxima and the lower lines in the $P_{3/2}$ and $R_{3/2}$ branches. In this way for HC_8H^+ (DC_8D^+) a

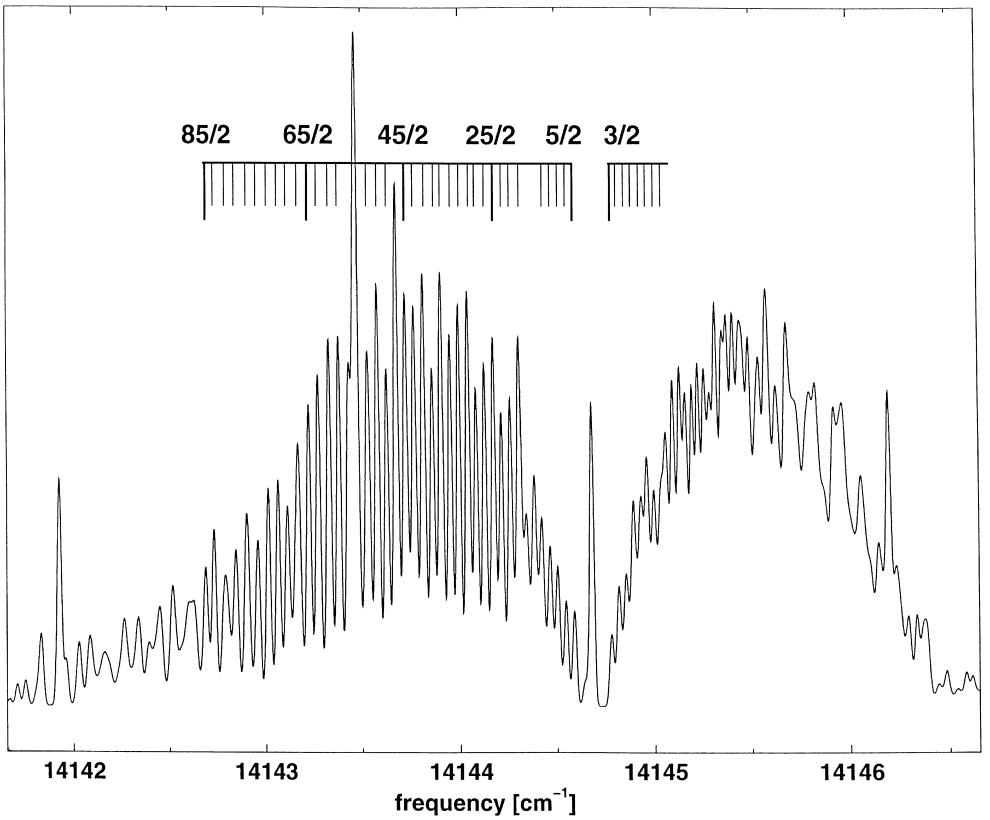

Fig. 2. Rotationally resolved CRD absorption spectrum of the $^2\Pi_{3/2} \leftarrow {}^2\Pi_{3/2}$ electronic origin band transition of HC_8H^+, recorded through a supersonic planar plasma ($T_{rot} \approx 15$ K). The rotational assignment is given. Some rotational lines were not observed because of overlap with C_2 transitions.

total of 139 (125) rotational transitions were assigned to the $A\,^2\Pi_{3/2} \leftarrow X\,^2\Pi_{3/2}$ subband. Most of the remaining transitions have been assigned to the $A\,^2\Pi_{1/2} \leftarrow X\,^2\Pi_{1/2}$ band. The line positions are given in Table 1 for HC_8H^+ and in Table 2 for DC_8D^+.

The rotational analysis of the data was performed by standard procedures using Pgopher [9]. The line positions were fit with an effective rotational Hamiltonian where both spin–orbit systems were considered at the same time. The band origin (ν_0), the rotational constant (B_0) and the centrifugal distortion constant (D_0) of both states were adjustable parameters. The line positions of the observed transitions could be fit to standard deviations that are significantly less than the observed linewidths. The resulting parameters are given in Table 3. Distortion constants are not listed here, as the uncertainties were found to be of the same order as the values themselves. The present data yield a value of $\Delta A = |A'' - A'| = \sim 3$ cm^{-1} comparable to values of 2.7 and 2.99 cm^{-1} for HC_4H^+ and HC_6H^+, respectively. It was not possible to determine the spin–orbit splittings independently. However, the value for A'' is expected to be similar to that of HC_6H^+, approximately -31 cm^{-1} [7].

The overall length of the tetraacetylene cation in both electronic states is determined by deriving the center-of-mass coordinates of the two hydrogen atoms using Kraichman's equations [10] for the HC_8H^+/DC_8D^+ pair. This yields a value of 12.05(2) [12.12(2)] Å in the $X\,^2\Pi_g[A\,^2\Pi_u]$ state.

Table 1
Frequencies (in cm^{-1}) and assignments for the $A\,^2\Pi_u \leftarrow X\,^2\Pi_g\ 0_0^0$ transition of HC_8H^+ and residuals (o-c) from the fit

J	Obs.	o-c[a]	J	Obs.	o-c[a]	J	Obs.	o-c[a]	J	Obs.	o-c[a]	J	Obs.	o-c[a]	J	Obs.	o-c[a]
$R_{3/2}$												$R_{1/2}$			$P_{1/2}$		
6.5	14 144.956	2	47.5	14 146.020	0	38.5	14 142.908	−1	79.5	14 140.330	−3	6.5	14 141.955	1	10.5	14 141.257	−3
7.5	14 144.989	0	48.5	14 146.039	1	39.5	14 142.855	0	81.5	14 140.188	1	8.5	14 141.024	1	14.5	14 141.090	3
9.5	14 145.058	1	50.5	14 146.070	−1	40.5	14 142.798	−2	82.5	14 140.112	−3	13.5	14 142.187	−1	16.5	14 140.990	−8
10.5	14 145.090	0	51.5	14 146.090	3	42.5	14 142.688	−1	83.5	14 140.043	1	15.5	14 142.250	−1	22.5	14 140.718	−4
11.5	14 145.124	1	53.5	14 146.117	1	43.5	14 142.637	5	84.5	14 139.964	−4	17.5	14 142.316	4	23.5	14 140.668	−6
12.5	14 145.152	−3	54.5	14 146.136	5	44.5	14 142.572	−3	85.5	14 139.895	0	19.5	14 142.374	3	29.5	14 140.377	−2
13.5	14 145.188	1				45.5	14 142.512	−7	88.5	14 139.670	0	21.5	14 142.431	2	30.5	14 140.330	1
14.5	14 145.218	0				46.5	14 142.457	−5	90.5	14 139.522	4	23.5	14 142.485	−1	31.5	14 140.276	−2
15.5	14 145.250	0	$P_{3/2}$			47.5	14 142.402	−2	91.5	14 139.442	0	25.5	14 142.533	−7	32.5	14 140.222	−5
16.5	14 145.282	1	2.5	14 144.59[b]	8	48.5	14 142.346	0	92.5	14 139.358	−7	28.5	14 142.615	−4	33.5	14 140.167	−8
17.5	14 145.313	3	3.5	14 144.55[b]	3	49.5	14 142.288	0	94.5	14 139.210	0	30.5	14 142.667	−2	36.5	14 140.018	1
18.5	14 145.341	1	4.5	14 144.51[b]	2	50.5	14 142.229	1	95.5	14 139.137	6	32.5	14 142.712	−6	39.5	14 139.851	−4
19.5	14 145.372	1	5.5	14 144.47[b]	3	51.5	14 142.167	−2	96.5	14 139.054	2	34.5	14 142.762	−3	40.5	14 139.797	−4
20.5	14 145.402	3	6.5	14 144.43[b]	1	52.5	14 142.109	0	97.5	14 138.971	−3	37.5	14 142.826	−5	41.5	14 139.739	−6
21.5	14 145.427	−1	7.5	14 144.384	1	53.5	14 142.048	0	98.5	14 138.896	2	45.5	14 142.988	−3	49.5	14 139.295	5
22.5	14 145.455	−1	8.5	14 144.343	2	54.5	14 141.983	−5	99.5	14 138.812	−2	48.5	14 143.039	−5	50.5	14 139.236	6
23.5	14 145.482	−2	9.5	14 144.31[b]	6	55.5	14 141.928	2	101.5	14 138.653	0	51.5	14 143.094	0	51.5	14 139.177	6
24.5	14 145.510	−1	10.5	14 144.258	−2	56.5	14 141.863	−2	102.5	14 138.566	−6				52.5	14 139.116	5
25.5	14 145.541	3	11.5	14 144.219	1	57.5	14 141.799	−5	104.5	14 138.408	0				53.5	14 139.056	4
26.5	14 145.565	0	12.5	14 144.174	−1	58.5	14 141.740	−1	105.5	14 138.325	0				54.5	14 138.995	4
27.5	14 145.593	2	13.5	14 144.130	−2	59.5	14 141.675	−3	106.5	14 138.244	1				55.5	14 138.935	6
28.5	14 145.617	1	14.5	14 144.080	−8	60.5	14 141.614	−1	107.5	14 138.162	3				56.5	14 138.874	6
29.5	14 145.642	1	15.5	14 144.05[b]	5	61.5	14 141.546	−5							57.5	14 138.814	7
30.5	14 145.668	2	16.5	14 144.000	1	62.5	14 141.485	−2							58.5	14 138.744	−0
31.5	14 145.691	1	17.5	14 143.954	0	63.5	14 141.424	2							59.5	14 138.688	6
32.5	14 145.715	1	18.5	14 143.903	−6	64.5	14 141.356	−1							62.5	14 138.499	7
33.5	14 145.739	1	19.5	14 143.87[b]	4	65.5	14 141.292	0							63.5	14 138.433	7
34.5	14 145.761	0	20.5	14 143.82[b]	5	66.5	14 141.228	1							65.5	14 138.302	5
35.5	14 145.782	−1	21.5	14 143.76[b]	6	67.5	14 141.160	0							66.5	14 138.231	0
36.5	14 145.804	−1	22.5	14 143.73[b]	8	68.5	14 141.092	−2							67.5	14 138.163	−2
37.5	14 145.827	0	23.5	14 143.675	1	69.5	14 141.026	0									
38.5	14 145.849	0	24.5	14 143.629	3	70.5	14 140.959	1									
39.5	14 145.866	−3	27.5	14 143.484	5	71.5	14 140.892	1									
40.5	14 145.888	−1	28.5	14 143.425	−4	72.5	14 140.816	−6									
41.5	14 145.911	1	29.5	14 143.376	−3	73.5	14 140.756	3									
42.5	14 145.931	2	31.5	14 143.275	−3	74.5	14 140.681	−3									
43.5	14 145.949	0	32.5	14 143.223	−3	75.5	14 140.616	2									
44.5	14 145.969	2	34.5	14 143.121	−2	76.5	14 140.544	−1									
45.5	14 145.988	2	35.5	14 143.071	1	77.5	14 140.472	−2									
46.5	14 146.003	0	36.5	14 143.012	−4	78.5	14 140.403	1									

[a] (o-c) in units of 10^{-3} cm^{-1}.
[b] Line positions from CRD spectrum.

Table 2
Frequencies (in cm^{-1}) and assignments for the A $^2\Pi_u \leftarrow$ X $^2\Pi_g$ 0_0^0 transition of DC_8D^+ and residuals (o-c) from the fit

J	Obs.	o-c[a]	J	Obs.	o-c[a]	J	Obs.	o-c[a]	J	Obs.	o-c[a]	J	Obs.	o-c[a]	J	Obs.	o-c[a]
$R_{3/2}$			$P_{3/2}$						$R_{1/2}$			$P_{1/2}$					
5.5	14 171.240	0	4.5	14 170.90[b]		54.5	14 168.523	−1	6.5	14 168.277	−5	3.5	14 167.906	2	63.5	14 165.015	2
6.5	14 171.270	−2	5.5	14 170.824	3	55.5	14 168.469	1	11.5	14 168.438	0	6.5	14 167.792	0	64.5	14 164.953	0
7.5	14 171.303	−1	6.5	14 170.781	−3	56.5	14 168.411	1	13.5	14 168.494	−3	8.5	14 167.720	3	65.5	14 164.890	−3
8.5	14 171.334	−2	8.5	14 170.705	−2	57.5	14 168.355	2	15.5	14 168.556	1	9.5	14 167.676	−2	66.5	14 164.831	−1
9.5	14 171.365	−1	9.5	14 170.68[b]		58.5	14 168.299	4	17.5	14 168.615	3	11.5	14 167.597	−3	67.5	14 164.772	2
10.5	14 171.397	−1	10.5	14 170.64[b]		59.5	14 168.238	1	19.5	14 168.666	−1	12.5	14 167.556	−3	68.5	14 164.708	−1
11.5	14 171.427	−1	11.5	14 170.591	0	60.5	14 168.179	1	21.5	14 168.721	0	13.5	14 167.522	2	69.5	14 164.645	−2
12.5	14 171.457	−1	12.5	14 170.553	2	61.5	14 168.120	1	23.5	14 168.774	2	14.5	14 167.477	−2	70.5	14 164.583	−2
13.5	14 171.486	−1	13.5	14 170.511	0	62.5	14 168.061	1	26.5	14 168.850	3	16.5	14 167.399	2	72.5	14 164.458	−2
14.5	14 171.515	−1	15.5	14 170.428	−1	63.5	14 168.001	1	28.5	14 168.893	−3	17.5	14 167.361	6	73.5	14 164.393	−2
15.5	14 171.544	−1	17.5	14 170.38[b]		64.5	14 167.941	1	30.5	14 168.944	2	19.5	14 167.272	2	74.5	14 164.329	−3
16.5	14 171.572	−1	18.5	14 170.303	−1	65.5	14 167.881	2	32.5	14 168.986	−1	20.5	14 167.228	1	75.5	14 164.269	2
17.5	14 171.600	−1	19.5	14 170.258	−3	66.5	14 167.817	−1	34.5	14 169.030	0	22.5	14 167.142	2	76.5	14 164.205	2
18.5	14 171.638	9	20.5	14 170.219	1	67.5	14 167.754	−3	35.5	14 169.050	−1	23.5	14 167.095	−1	77.5	14 164.139	1
19.5	14 171.656	0	21.5	14 170.172	−3	68.5	14 167.694	−1	36.5	14 169.095	3	25.5	14 167.007	1	78.5	14 164.071	−1
20.5	14 171.684	1	23.5	14 170.089	2	69.5	14 167.629	−4	40.5	14 169.152	2	26.5	14 166.961	−1	79.5	14 164.004	−3
21.5	14 171.711	2	24.5	14 170.043	1	70.5	14 167.571	0	42.5	14 169.188	1	30.5	14 166.777	0			
22.5	14 171.736	1	25.5	14 169.994	−4	71.5	14 167.504	−3	43.5	14 169.210	4	32.5	14 166.680	−2			
23.5	14 171.762	1	26.5	14 169.948	−5	72.5	14 167.443	−1	45.5	14 169.241	1	33.5	14 166.633	−1			
24.5	14 171.787	1	27.5	14 169.907	0	73.5	14 167.381	0	46.5	14 169.257	0	35.5	14 166.536	−1			
25.5	14 171.812	1	28.5	14 169.859	−1	74.5	14 167.317	1	49.5	14 169.301	−4	36.5	14 166.487	−1			
26.5	14 171.836	0	29.5	14 169.814	0	75.5	14 167.253	2				38.5	14 166.390	2			
27.5	14 171.859	−1	30.5	14 169.772	5	76.5	14 167.187	0				39.5	14 166.335	−2			
28.5	14 171.883	0	31.5	14 169.720	0	77.5	14 167.120	−2				40.5	14 166.286	−1			
29.5	14 171.906	−1	32.5	14 169.669	−3	78.5	14 167.054	−2				41.5	14 166.234	−1			
30.5	14 171.929	0	33.5	14 169.62[b]		79.5	14 166.990	0				43.5	14 166.135	2			
31.5	14 171.952	0	34.5	14 169.577	1	80.5	14 166.925	1				44.5	14 166.082	2			
32.5	14 171.974	0	35.5	14 169.528	2	81.5	14 166.853	−3				46.5	14 165.977	3			
33.5	14 171.995	−1	36.5	14 169.476	−1	82.5	14 166.790	0				47.5	14 165.921	0			
34.5	14 172.018	0	37.5	14 169.428	0	83.5	14 166.727	5				48.5	14 165.868	1			
35.5	14 172.039	0	38.5	14 169.380	2	84.5	14 166.653	−1				50.5	14 165.760	2			
36.5	14 172.059	0	39.5	14 169.330	3	85.5	14 166.587	1				51.5	14 165.705	2			
37.5	14 172.079	0	40.5	14 169.278	2	86.5	14 166.517	0				52.5	14 165.643	−5			
38.5	14 172.098	−1	41.5	14 169.225	−1	87.5	14 166.448	1				53.5	14 165.590	−2			
39.5	14 172.116	−2	42.5	14 169.170	−4	88.5	14 166.377	−2				54.5	14 165.535	−1			
40.5	14 172.137	0	43.5	14 169.120	−2	89.5	14 166.309	1				55.5	14 165.478	−1			
41.5	14 172.154	−2	44.5	14 169.071	1	90.5	14 166.238	0				56.5	14 165.423	1			
42.5	14 172.174	1	45.5	14 169.014	−2	91.5	14 166.165	−2				57.5	14 165.365	0			
43.5	14 172.191	−1	46.5	14 168.965	1	92.5	14 166.097	0				58.5	14 165.306	−1			

Table 2 (Continued)

J	Obs.	o-c[a]	J	Obs.	o-c[a]	J	Obs.	o-c[a]	J	Obs.	o-c[a]	J	Obs.	o-c[a]
$R_{3/2}$			$P_{3/2}$						$R_{1/2}$			$P_{1/2}$		
44.5	14 172.209	0	47.5	14 168.913	3	93.5	14 166.028	3				59.5	14 165.253	3
			48.5	14 168.853	−3	94.5	14 165.950	−3				60.5	14 165.193	2
			49.5	14 168.799	−2	95.5	14 165.879	−2				61.5	14 165.134	2
			50.5	14 168747	0	96.5	14 165.814	5				62.5	14 165.075	2
			51.5	14 168.695	3	97.5	14 165.737	2						
			52.5	14 168.639	3									
			53.5	14 168.582	2									

[a] (o-c) in units of 10^{-3} cm^{-1}.
[b] Line positions from CRD spectrum (not included in the fit).

Table 3
Molecular constants (in cm^{-1}) of HC_8H^+ and DC_8D^+ in the $X\,^2\Pi_g$ and $A\,^2\Pi_u$ states, derived from the analyses of the FM spectra. N is the number of lines used in the fit; o-c is the observed minus calculated standard deviation of the fit (in cm^{-1})[a]

	HC_8H^+	DC_8D^+
	$X\,^2\Pi_g$ state	
B''_0	0.019 077 9(93)	0.017 647 6(64)
A''_0	−31[b]	−31[b]
	$A\,^2\Pi_u$ state	
B'_0	0.018 867 3(94)	0.017 451 7(64)
ΔA	−3.00(1)	−2.99(1)
ν_0	14 143.18148(47)	14 169.52434(30)
N	186	205
o-c	0.0034	0.0021

[a] One standard deviation given in parentheses.
[b] From Ref. [7].

Acknowledgements

This work has been supported by the Swiss National Science Foundation, project number 20-55285.98.

References

[1] H. Schüler, L. Reinbeck, Z. Naturforsch. 7a (1952) 285.
[2] J.H. Callomon, Can. J. Phys. 34 (1956) 1046.
[3] M. Allan, E. Kloster–Jensen, J.P. Maier, Chem. Phys. 7 (1976) 11.
[4] R. Kuhn, J.P. Maier, M. Ochsner, Mol. Phys. 59 (1986) 441.
[5] J. Lecoultre, J.P. Maier, M. Ochsner, W. Zambach 88 (1984) 5176.
[6] M. Allan, E. Heilbronner, E. Kloster–Jensen, J.P. Maier, Chem. Phys. Lett. 41 (1976) 228.
[7] W.E. Sinclair, D. Pfluger, H. Linnartz, J.P. Maier, J. Chem. Phys. 110 (1999) 296.
[8] T. Motylewski, H. Linnartz, Rev. Sci. Instr. 70 (1999) 1305.
[9] C.M. Western, School of Chemistry, University of Bristol, UK, PGOPHER, vol. 3, 1994, p. 73.
[10] J. Kraitchman, Am. J. Phys. 21 (1953) 17.